

# Lawrence Berkeley National Laboratory

## Chemical Sciences

### Title

A Thorium Metal-Organic Framework with Outstanding Thermal and Chemical Stability

### Permalink

<https://escholarship.org/uc/item/0p4915fp>

### Journal

Chemistry - A European Journal, 25(29)

### ISSN

0947-6539

### Authors

Carter, Korey P  
Ridenour, J August  
Kalaj, Mark  
[et al.](#)

### Publication Date

2019-05-23

### DOI

10.1002/chem.201901610

Peer reviewed

## Actinides

## A Thorium Metal-Organic Framework with Outstanding Thermal and Chemical Stability

Korey P. Carter,<sup>[a, b]</sup> J. August Ridenour,<sup>[a]</sup> Mark Kalaj,<sup>[a, c]</sup> and Christopher L. Cahill\*<sup>[a]</sup>

**Abstract:** A new thorium metal-organic framework (MOF), Th(OBA)<sub>2</sub>, where OBA is 4,4'-oxybis(benzoic) acid, has been synthesized hydrothermally in the presence of a range of nitrogen-donor coordination modulators. This Th-MOF, described herein as GWMOF-13, has been characterized by single-crystal and powder X-ray diffraction, as well as through a range of techniques including gas sorption, thermogravimetric analysis (TGA), solid-state UV/Vis and luminescence spectroscopy. Single-crystal X-ray diffraction analysis of GWMOF-13 reveals an interesting, high symmetry (cubic *Ia $\bar{3}d$* ) structure, which yields a novel **srs-a** topology. Most notably, TGA analysis of GWMOF-13 reveals framework stability to 525 °C, matching the thermal stability benchmarks of the UiO-66 series MOFs and zeolitic imidazolate frameworks (ZIFs), and setting a new standard for thermal stability in f-block based MOFs.

Metal-organic frameworks (MOFs) represent an expansive family of compounds that have been developed for a variety of applications including gas sorption and separations,<sup>[1]</sup> catalysis,<sup>[2]</sup> and biomedicine.<sup>[3]</sup> MOFs have also exhibited significant promise for nuclear fuel cycle applications including uranium extraction,<sup>[4]</sup> Kr/Xe capture,<sup>[5]</sup> I<sub>2</sub> sorption,<sup>[6]</sup> and more recently, as hierarchical materials for long-term waste immobilization.<sup>[7]</sup> The multitude of inorganic secondary building units (SBUs) and nearly limitless variety of polytopic organic linkers has led, so far, to thousands of MOF architectures with a wide array of shapes, pore sizes, and chemical functionalities. Despite the significance and continually growing interest in this class of materials, synthesis of MOFs built from actinide metal centers, and in particular Th<sup>IV</sup>, represents an underdeveloped area of study.<sup>[8]</sup>

Fifteen years ago O'Hare and colleagues prepared the first Th-MOF,<sup>[9]</sup> and since then, only a handful of additional examples have been synthesized.<sup>[5b, 10]</sup> As thorium is capable of exhibiting a greater variety of coordination numbers and more diverse coordination environments than other high charge density tetravalent metal cations (e.g., Zr<sup>IV</sup>, Hf<sup>IV</sup>, Ce<sup>IV</sup>),<sup>[11]</sup> there are distinct opportunities to prepare new Th-MOFs which display elevated thermal and hydrolytic stability, which have no transition metal or lanthanide analogues. Beyond new materials exploration, MOF synthesis with Th<sup>IV</sup> also represents a forum to explore Th<sup>IV</sup> hydrolysis further, where studies have demonstrated a dependence on both pH and the relative nature of the ligand(s).<sup>[12]</sup> Additional insights into Th<sup>IV</sup> hydrolysis, and how it can be harnessed, are thus appropriate for developing a more thorough understanding of the chemical behavior of thorium, which is increasingly relevant as Th<sup>IV</sup> finds more applications in both the nuclear energy and nuclear medicine arenas.<sup>[13]</sup>

After a decade hiatus from MOF synthesis,<sup>[14]</sup> herein we re-initiate our efforts by pairing Th<sup>IV</sup> with 4,4'-oxybis(benzoic) acid (OBA) to produce [Th(OBA)<sub>2</sub>], which we will refer to as GWMOF-13 hereafter. 4,4'-oxybis(benzoic) acid (OBA) is a flexible V-shaped ligand comprised of two benzoic acid groups bridged together at the *para* position by an sp<sup>3</sup> ether oxygen atom, which has been extensively utilized in the synthesis of new luminescent Ln<sup>III</sup> coordination polymers (CPs) and MOFs.<sup>[15]</sup> OBA has a propensity to yield helical chain SBUs in CPs and MOFs, and this SBU is known to enhance structural robustness in MOFs.<sup>[16]</sup> By combining Th<sup>IV</sup> and OBA to yield GWMOF-13, a Th-MOF assembled from interpenetrating helical chains, it was our aim to synergistically combine ideal characteristics of both metal and ligand to generate a potential Th<sup>IV</sup>-based hierarchical waste form,<sup>[7]</sup> which could serve as a model for other An<sup>IV</sup> species. GWMOF-13 was found to display excellent thermal stability, maintaining structural integrity past 500 °C, and the MOF is also stable in boiling water, as well as in a wide-range of polar and non-polar organic solvents, demonstrating the robust nature of this new Th<sup>IV</sup> material.

Single-crystal X-ray crystallography analysis reveals that GWMOF-13, [Th(OBA)<sub>2</sub>], crystallizes in the cubic space group *Ia $\bar{3}d$* , and features a single crystallographically-unique thorium cation that has adopted square antiprismatic coordination geometry. Each Th<sup>IV</sup> cation in GWMOF-13 is bound to eight OBA ligands, one of which is crystallographically unique, and all of which adopt *syn,syn- $\eta^1$ : $\eta^1$ : $\mu_2$*  bridging conformations (Figure 1 A). Th1–O bonds to OBA ligands (O1–O4) are at an average distance of 2.386 Å, and OBA ligands link Th<sup>IV</sup> metal cen-

[a] Dr. K. P. Carter, J. A. Ridenour, M. Kalaj, Prof. Dr. C. L. Cahill  
Department of Chemistry, The George Washington University  
Washington, D.C. 20052 (USA)  
E-mail: cahill@gwu.edu

[b] Dr. K. P. Carter  
Chemical Sciences Division, Lawrence Berkeley National Laboratory  
Berkeley, CA 94720 (USA)

[c] M. Kalaj  
Department of Chemistry and Biochemistry, University of California  
San Diego, La Jolla, CA 92093 (USA)

Supporting information and the ORCID identification number(s) for the author(s) of this article can be found under:  
<https://doi.org/10.1002/chem.201901610>

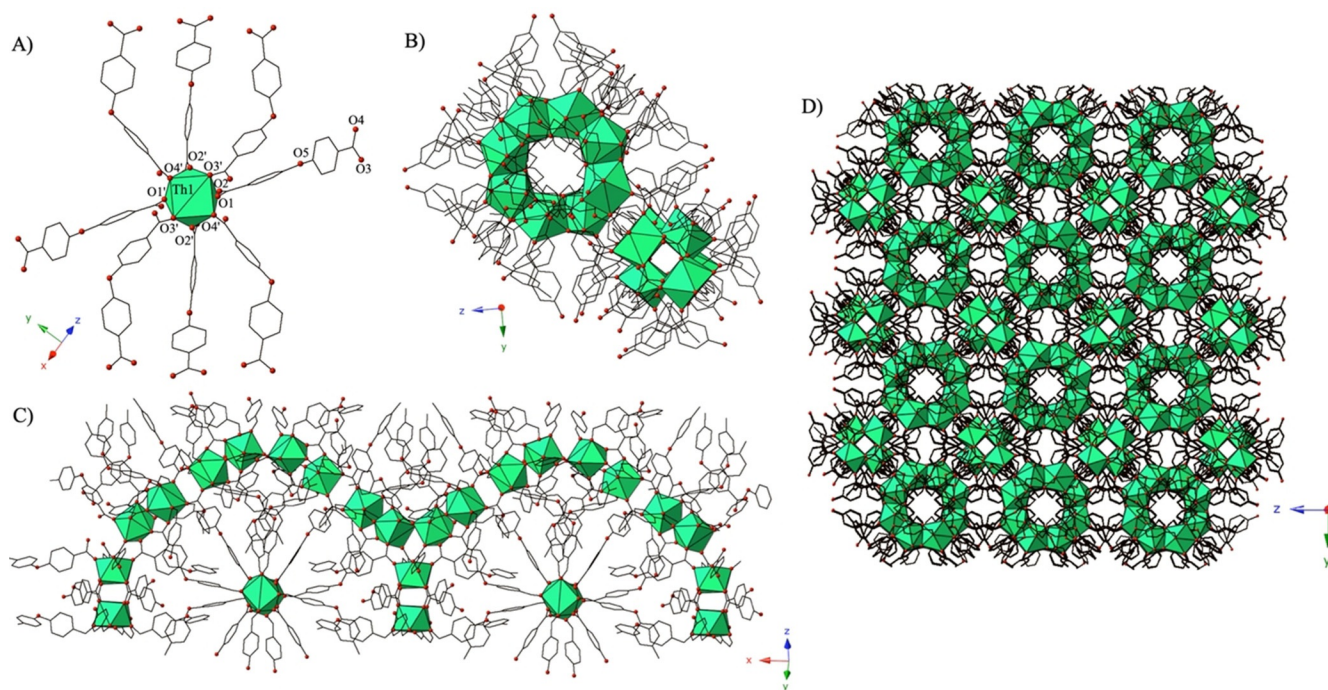


**Figure 1.** A) Polyhedral representation highlighting the local coordination environment of  $\text{Th}^{4+}$  cations in GWMOF-13. Green polyhedra are  $\text{Th}^{\text{IV}}$  centers, whereas red spheres are oxygen atoms. All H atoms have been omitted for clarity. B) One helical chain of GWMOF-13 shown in (100) plane illustrating formation of two, unique square 1D channels. C) Side view in (010) plane of helical chain highlighting hub-and-spoke nature of chains of GWMOF-13. D) 3D framework structure of GWMOF-13 shown in (100) plane.

ters into helical hub-and-spoke like chains, which generate square 1D channels with diameters of 3.5 and 1.4 Å, respectively (Figures 1B and C). In between each square 1D channel of GWMOF-13 are 1D ellipsoidal channels with dimensions of ca.  $10.85 \times 7.2$  Å that are filled by hydrogen atoms from OBA ligands (Figure 1D). Helical chains of GWMOF-13 assemble into a 3D framework with a solvent accessible volume of 15.6% (of the total volume) as estimated by PLATON (Figure 1D).<sup>[17]</sup>

The 3D framework of GWMOF-13 is both elegant and highly complex (Figure 2). In simplistic terms the structure can be considered as two interwoven nets that are cross-linked by an OBA ligand. Topological analysis indicates that the two uninodal nets have point symmetry  $3^{25}.4^{60}.5^{20}$ , and are one of the first examples of nets with (4,8)-c topology.<sup>[18]</sup> Alternatively, if the single 4-coordinate (4-c) representation of the ligand is reduced to two 3-c nodes,<sup>[19]</sup> then the nets can be described as (3,3,8)-c, which is also a new topology. The simplest description of the GWMOF-13, however, is obtained by visualizing the  $\text{Th}^{\text{IV}}$  cations as nodes, and replacing the organic anions as “struts” (Figure 2). In this case, the 2-fold related nets of GWMOF-13 can be described as having **srs-a** (augmented **srs**) topology, and these two interpenetrated **srs-a** nets are then bridged by ligand anions to form a single net.

The density of GWMOF-13 limits its permanent porosity, as demonstrated by adsorption studies with  $\text{CO}_2$  at room temperature and  $\text{N}_2$  and  $\text{H}_2$  at 77 K after evacuation under high vacuum overnight at 105 °C. GWMOF-13 was found to be a microporous material as indicated by the isotherms for all three adsorbates (Figures S1–S3, Supporting Information), yet

Brunauer–Emmett–Teller (BET) surface area values for GWMOF-13 are small ( $0.256 \text{ mmol g}^{-1} \text{ CO}_2$ ,  $5.0 \text{ m}^2 \text{ g}^{-1} \text{ N}_2$ , and  $11.94 \text{ cm}^3 \text{ g}^{-1} \text{ H}_2$ ), which suggests that porosity toward the three gases is limited in the applied pressure ranges.

Thermogravimetric analysis (TGA) of GWMOF-13 demonstrated that the framework is very robust, as decomposition did

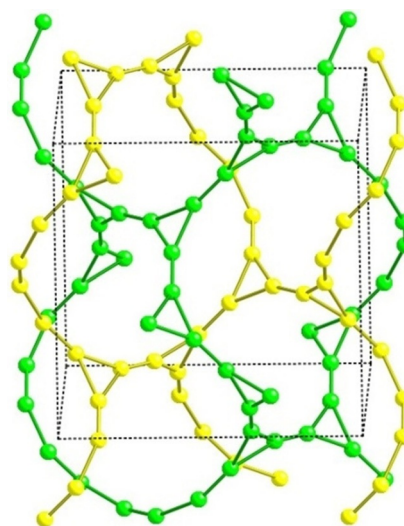


**Figure 2.** The **srs-a** net of GWMOF-13. Spheres represent thorium cation nodes. The two interwoven nets are shown in yellow and green. Struts are drawn between nodes that are bridged by OBA ligands in *syn,syn-η¹:η¹:μ₂* configuration. For clarity no struts have been included to represent the ligands that cross-link the two nets. The cubic unit cell is shown as dashed lines.

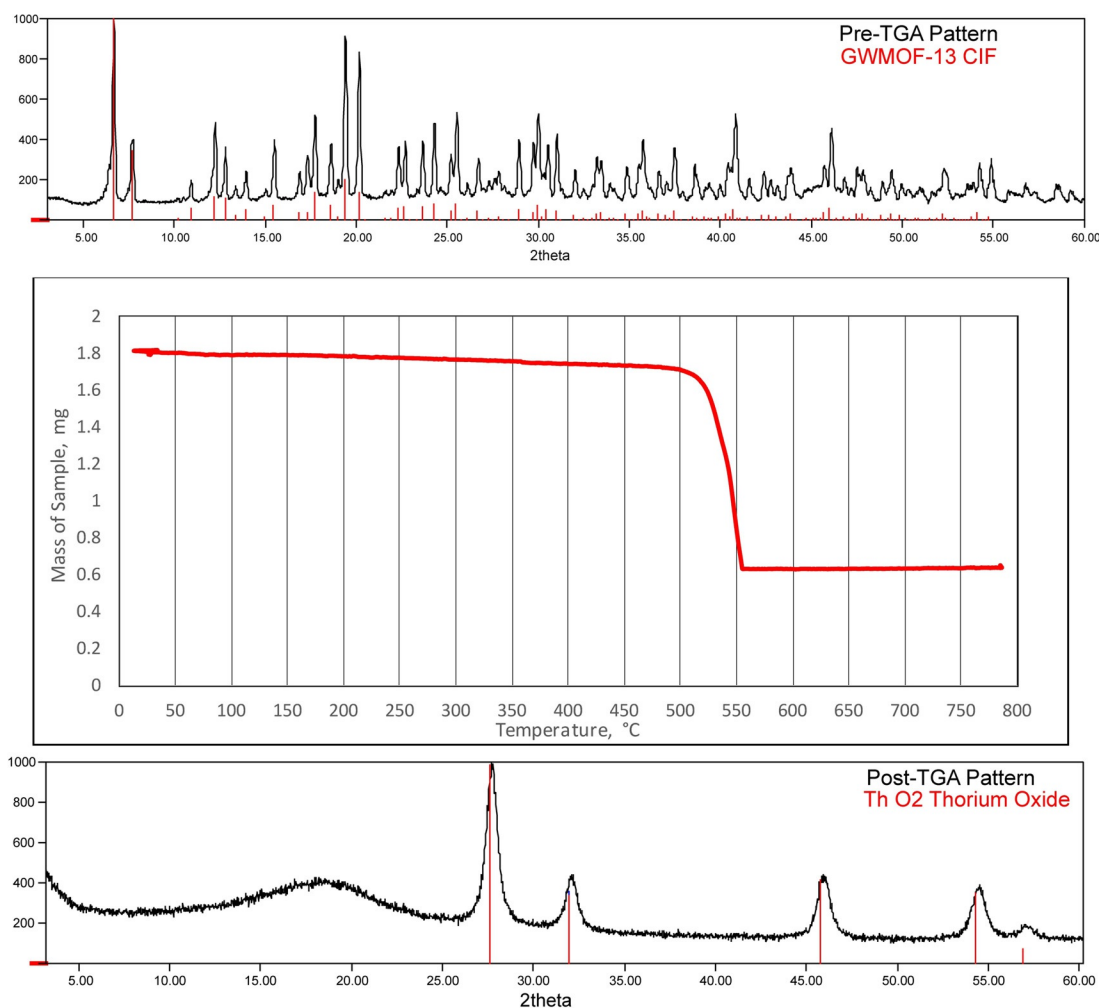


**Figure 3.** (Top) Pre-TGA PXRD pattern of GWMOF-13 with calculated pattern of GWMOF-13 overlaid in red. (Middle) Thermogravimetric analysis (TGA) curve of GWMOF-13. (Bottom) Post-TGA PXRD pattern of GWMOF-13 with calculated pattern of ThO<sub>2</sub> overlaid in red.

not begin until above 500 °C (Figure 3). The corresponding ≈ 65% weight loss is in good agreement with the calculated (68.8%) weight percent of OBA, with the remaining ≈ 30% corresponding to thorium oxide (confirmed by PXRD) (Figure 3). Notably, we observe the same TGA results for fresh samples and those that have been aged (for more than a year), indicating that the thermal stability of GWMOF-13 is not affected over time. In general, thermal stability of MOFs is usually limited to 350–400 °C,<sup>[20]</sup> with a few examples of frameworks that are stable above ca. 500 °C, such as UiO-66 and zeolitic imidazolate frameworks (ZIFs),<sup>[20–21]</sup> setting the standard for MOF thermal stability, which has been matched here by GWMOF-13.

To verify the chemical stability of GWMOF-13, as synthesized samples were soaked in boiling water, strongly acidic aqueous solutions (6 M HCl, 6 M HNO<sub>3</sub>), and strongly basic aqueous solution (6 M NaOH) for one day at room temperature. The PXRD pattern of the GWMOF-13 sample after being treated in boiling water matches well with that of the pristine sample (Figure S4A, Supporting Information), whereas we observe a breakdown of the MOF in strongly acidic and strongly basic media. In both 6 M HCl and 6 M HNO<sub>3</sub>, PXRD confirms the presence of free OBA (Figures S4B and C), whereas in 6 M NaOH,

crystallinity is significantly diminished, and we were unable to identify the final post-soaking product(s) (Figure S4D). Additionally, we explored the stability of GWMOF-13 in a range of polar and nonpolar organic solvents and after soaking times of one day, GWMOF-13 was found to be completely insoluble in all solvents tested (acetone, THF, DMF, DMSO, methanol, ethanol, acetonitrile, diethyl ether, dichloromethane, cyclohexane, and benzene) with PXRD patterns matching that of the pristine sample in all instances (Figure S5).

Finally, the solid-state spectroscopic properties of GWMOF-13 were investigated as it is well-known that luminescence in Th<sup>IV</sup> materials is entirely a result of ligand fluorescence processes. Figure S6 (Supporting Information) shows the UV/Vis and luminescence spectra of both OBA and GWMOF-13, and both spectra provide insight into how ligand insertion within the MOF scaffold affects ligand absorption and emission pathways. In the UV/Vis (Figure S6 Left), we note a small redshift in the spectrum of GWMOF-13, yet the more interesting observation is the similar shape of the two spectra, as this indicates that ligand absorption transitions are only weakly perturbed by insertion into the GWMOF-13 framework.<sup>[22]</sup> Similar trends are also noted in the luminescence spectra of OBA and GWMOF-



13 (Figure S6 Right), and a look at the normalized absorbance and luminescence spectra of GWMOF-13 (Figure S6 Bottom) displays only a limited amount of overlap, suggestive of minimal self-absorption effects.<sup>[10g]</sup>

The synthesis and crystal structure of a new thorium(IV)-MOF, GWMOF-13, featuring 4,4'-oxybis(benzoic) acid is reported, and the resulting *srs-a* topology has been detailed. GWMOF-13 demonstrates excellent thermal stability up to 525 °C, and extended aging of the MOF is not found to impact framework thermal or chemical properties. Soaking experiments revealed that GWMOF-13 is also stable in a full range of polar and nonpolar organic solvents and can withstand twenty-four-hour treatment in boiling water. Only in extreme conditions, such as strongly acidic or basic media (6 M HCl, 6 M HNO<sub>3</sub>, or 6 M NaOH), do we observe framework decomposition resulting in either free OBA in acidic media or complete breakdown of GWMOF-13 in 6 M NaOH. While GWMOF-13 demonstrates some limitations in terms of functioning as a potential waste form for long-term immobilization efforts, it does highlight a path forward for MOF synthesis with this end goal in mind, and efforts exploring new, similar ligands to OBA with both Th<sup>IV</sup> and other tetravalent actinide species are in progress.

## Experimental Section

GWMOF-13 was synthesized by hydrothermal methods at autogeneous pressure in a 23 mL Teflon-lined Parr bomb. There are many synthetic routes to generate single crystals of GWMOF-13 over the pH range 1–5; thus we will only outline the (hydrothermal) protocol for optimal single-crystal growth. A mixture containing 55 mg (0.10 mmol) of Th(NO<sub>3</sub>)<sub>4</sub>·4H<sub>2</sub>O, 52 mg (0.20 mmol) of 4,4'-oxybis(benzoic) acid, 36 mg (0.20 mmol) of 1,10-phenanthroline, and 1.5 mL (83.3 mmol) of water was placed in a Parr autoclave and then heated statically at 120 °C for 72 h. Upon removal from the oven, the sample was allowed to cool over four hours, and the Parr bomb opened after approximately 16 h. The solution and solid products were both colorless and after washing three times with water and ethanol, the bulk product was dried at ambient conditions, yielding large, cubic crystals, which were unusually robust. More specifically, crystals of GWMOF-13 that were stuck together could not be separated by application of a small amount of pressure, as is common for inorganic hybrid materials and MOFs. Instead, separating crystals required chiseling them apart, in a manner more reminiscent of a mining process.

The inclusion of a *N*-donor species (1,10-phenanthroline, 2,2'-bipyridine, or 2,2':6',2"-terpyridine) in the reaction mixture was originally part of efforts to extend the "cap and link" approach our group has developed for promoting via non-covalent interactions in Ln<sup>III</sup> and UO<sub>2</sub><sup>2+</sup> hybrid materials to Th<sup>IV</sup>.<sup>[23]</sup> While these efforts were unsuccessful, we did find the inclusion of *N*-donor species to be necessary to yield single crystals of GWMOF-13, which can be explained by the coordination modulator concept introduced by Kitagawa et al.,<sup>[24]</sup> wherein a capping ligand (or reagent) is introduced to generate a competitive situation in solution that regulates the rate of framework extension and crystal growth. This strategy was particularly valuable herein as Th<sup>IV</sup> is known to produce poorly crystalline material,<sup>[25]</sup> and in the absence of *N*-donor modulators, GWMOF-13 is produced only as a fine, microcrystalline powder.

The Supporting Information contains further experimental details, additional figures, gas sorption data for GWMOF-13, solid-state UV/Vis and luminescence spectra for GWMOF-13, PXRD spectra of GWMOF-13 after treatment in aqueous, acidic, basic, and organic media, PXRD and IR spectra of GWMOF-13 made with different *N*-donor modulators, and X-ray crystallographic data in CIF format for GWMOF-13. CCDC 1902331 contains the supplementary crystallographic data for this paper. These data are provided free of charge by The Cambridge Crystallographic Data Centre.

## Acknowledgements

This study was supported by the U. S. Department of Energy (DOE)-Chemical Sciences, Geosciences and Biosciences Division, Office of Science, Office of Basic Energy Sciences, Heavy Elements Program, under grant number DE-FG02-05ER15736. The authors would like to thank Professor Michael Wagner and the Wagner group at The George Washington University for TGA instrument time, Ms. Jennifer Szymanowski for assistance with IR measurements, which were collected at the University of Notre Dame University Energy Center, and Professor Seth Cohen at UCSD for facilitating gas sorption data collection. We also thank Dr. Elinor Spencer and Professor Nancy Ross at Virginia Tech University for valuable conversations related to topological analysis of GWMOF-13. M.K. is currently supported by the Department of Defense (DoD) through the National Defense Science and Engineering Graduate (NDSEG) Fellowship Program.

## Conflict of interest

The authors declare no conflict of interest.

**Keywords:** actinides · carboxylate ligands · metal-organic frameworks · X-ray diffraction

- [1] a) K. Sumida, D. L. Rogow, J. A. Mason, T. M. McDonald, E. D. Bloch, Z. R. Herm, T.-H. Bae, J. R. Long, *Chem. Rev.* **2012**, *112*, 724–781; b) M. S. Denry Jr., J. C. Moreton, L. Benz, S. M. Cohen, *Nat. Rev. Mater.* **2016**, *1*, 16078; c) H. Kim, S. R. Rao, E. A. Kapustin, L. Zhao, S. Yang, O. M. Yaghi, E. N. Wang, *Nat. Commun.* **2018**, *9*, 1191; d) R.-B. Lin, S. Xiang, H. Xing, W. Zhou, B. Chen, *Coord. Chem. Rev.* **2019**, *378*, 87–103.
- [2] a) J. Liu, L. Chen, H. Cui, J. Zhang, L. Zhang, C.-Y. Su, *Chem. Soc. Rev.* **2014**, *43*, 6011–6061; b) S. M. J. Rogge, A. Bavykina, J. Hajek, H. Garcia, A. I. Olivios-Suarez, A. Sepúlveda-Escribano, A. Vimont, G. Clet, P. Bazin, F. Kapteijn, M. Daturi, E. V. Ramos-Fernandez, F. X. Llabrés i Xamena, V. Van Speybroeck, J. Gascon, *Chem. Soc. Rev.* **2017**, *46*, 3134–3184; c) S. Yuan, L. Feng, K. Wang, J. Pang, M. Bosch, C. Lollar, Y. Sun, J. Qin, X. Yang, P. Zhang, Q. Wang, L. Zou, Y. Zhang, L. Zhang, Y. Fang, J. Li, H.-C. Zhou, *Adv. Mater.* **2018**, *30*, 1704303.
- [3] a) J. Della Rocca, D. Liu, W. Lin, *Acc. Chem. Res.* **2011**, *44*, 957–968; b) Y. Chen, P. Li, J. A. Modica, R. J. Drout, O. K. Farha, *J. Am. Chem. Soc.* **2018**, *140*, 5678–5681; c) I. Abánades Lázaro, S. Haddad, J. M. Rodrigo-Muñoz, R. J. Marshall, B. Sastre, V. del Pozo, D. Fairen-Jimenez, R. S. Forgan, *ACS Appl. Mater. Interfaces* **2018**, *10*, 31146–31157.
- [4] M. Carboni, C. W. Abney, S. Liu, W. Lin, *Chem. Sci.* **2013**, *4*, 2396–2402.
- [5] a) D. Banerjee, C. M. Simon, A. M. Plonka, R. K. Motkuri, J. Liu, X. Chen, B. Smit, J. B. Parise, M. Haranczyk, P. K. Thallapally, *Nat. Commun.* **2016**, *7*, 11831; b) Y. Wang, W. Liu, Z. Bai, T. Zheng, M. A. Silver, Y. Li, Y. Wang, X. Wang, J. Diwu, Z. Chai, S. Wang, *Angew. Chem. Int. Ed.* **2018**, *57*, 5783–5787; *Angew. Chem.* **2018**, *130*, 5885–5889.

- [6] a) C. Falaise, C. Volkringer, J. Facqueur, T. Bousquet, L. Gasnot, T. Loiseau, *Chem. Commun.* **2013**, 49, 10320–10322; b) D. Banerjee, X. Chen, S. S. Lobanov, A. M. Plonka, X. Chan, J. A. Daly, T. Kim, P. K. Thallapally, J. B. Parise, *ACS Appl. Mater. Interfaces* **2018**, 10, 10622–10626.
- [7] H.-C. zur Loye, T. Besmann, J. Amoroso, K. Brinkman, A. Grandjean, C. H. Henager, S. Hu, S. T. Misture, S. R. Phillpot, N. B. Shustova, H. Wang, R. J. Koch, G. Morrison, E. Dolgoplova, *Chem. Mater.* **2018**, 30, 4475–4488.
- [8] E. A. Dolgoplova, A. M. Rice, N. B. Shustova, *Chem. Commun.* **2018**, 54, 6472–6483.
- [9] J.-Y. Kim, A. J. Norquist, D. O'Hare, *J. Am. Chem. Soc.* **2003**, 125, 12688–12689.
- [10] a) K. M. Ok, J. Sung, G. Hu, R. M. J. Jacobs, D. O'Hare, *J. Am. Chem. Soc.* **2008**, 130, 3762–3763; b) K. M. Ok, D. O'Hare, *Dalton Trans.* **2008**, 5560–5562; c) C. Falaise, J.-S. Charles, C. Volkringer, T. Loiseau, *Inorg. Chem.* **2015**, 54, 2235–2242; d) Y. Li, Z. Weng, Y. Wang, L. Chen, D. Sheng, Y. Liu, J. Diwu, Z. Chai, T. E. Albrecht-Schmitt, S. Wang, *Dalton Trans.* **2015**, 44, 20867–20873; e) E. A. Dolgoplova, O. A. Ejegbavwo, C. R. Martin, M. D. Smith, W. Setyawan, S. G. Karakalos, C. H. Henager, H.-C. zur Loye, N. B. Shustova, *J. Am. Chem. Soc.* **2017**, 139, 16852–16861; f) Y. Li, Z. Yang, Y. Wang, Z. Bai, T. Zheng, X. Dai, S. Liu, D. Gui, W. Liu, M. Chen, L. Chen, J. Diwu, L. Zhu, R. Zhou, Z. Chai, T. E. Albrecht-Schmitt, S. Wang, *Nat. Commun.* **2017**, 8, 1354; g) J. Andreo, E. Priola, G. Alberto, P. Benzi, D. Marabello, D. M. Proserpio, C. Lamberti, E. Diana, *J. Am. Chem. Soc.* **2018**, 140, 14144–14149; h) P. Li, S. Goswami, K.-I. Otake, X. Wang, Z. Chen, S. L. Hanna, O. K. Farha, *Inorg. Chem.* **2019**, 58, 3586–3590.
- [11] C. D. Tutson, A. E. V. Gorden, *Coord. Chem. Rev.* **2017**, 333, 27–43.
- [12] a) K. E. Knope, L. Soderholm, *Chem. Rev.* **2013**, 113, 944–994; b) P. L. Zanonato, P. Di Bernardo, Z. Zhang, Y. Gong, G. Tian, J. K. Gibson, L. Rao, *Dalton Trans.* **2016**, 45, 12763–12771; c) C. Falaise, K. Kozma, M. Nyman, *Chem. Eur. J.* **2018**, 24, 14226–14232.
- [13] a) L. S. Natrajan, A. N. Swinburne, M. B. Andrews, S. Randall, S. L. Heath, *Coord. Chem. Rev.* **2014**, 266–267, 171–193; b) G. J. P. Deblonde, T. D. Lohrey, C. H. Booth, K. P. Carter, B. F. Parker, Å. Larsen, R. Smeets, O. B. Ryan, A. S. Cuthbertson, R. J. Abergel, *Inorg. Chem.* **2018**, 57, 14337–14346.
- [14] a) C. L. Cahill, D. T. de Lill, M. Frisch, *CrystEngComm* **2007**, 9, 15–26; b) D. T. de Lill, C. L. Cahill, *Cryst. Growth Des.* **2007**, 7, 2390–2393.
- [15] a) Y. Luo, Y. Zheng, G. Calvez, S. Freslon, K. Bernot, C. Daiguebonne, T. Roisnel, O. Guillou, *CrystEngComm* **2013**, 15, 706–720; b) D. Ma, X. Li, R. Huo, *J. Mater. Chem. C* **2014**, 2, 9073–9076; c) Y. Li, N. Wang, Y.-J. Xiong, Q. Cheng, J.-F. Fang, F.-F. Zhu, Y. Long, S.-T. Yue, *New J. Chem.* **2015**, 39, 9872–9878; d) D. Yang, Y. Tian, W. Xu, X. Cao, S. Zheng, Q. Ju, W. Huang, Z. Fang, *Inorg. Chem.* **2017**, 56, 2345–2353.
- [16] Z. Yao, Z. Zhang, L. Liu, Z. Li, W. Zhou, Y. Zhao, Y. Han, B. Chen, R. Krishna, S. Xiang, *Chem. Eur. J.* **2016**, 22, 5676–5683.
- [17] A. L. Spek, *J. Appl. Crystallogr.* **2003**, 36, 7–13.
- [18] V. A. Blatov, A. P. Shevchenko, V. N. Serezhkin, *J. Struct. Chem.* **1994**, 34, 820–822.
- [19] M. Li, D. Li, M. O'Keeffe, O. M. Yaghi, *Chem. Rev.* **2014**, 114, 1343–1370.
- [20] J. H. Cavka, S. Jakobsen, U. Olsbye, N. Guillou, C. Lamberti, S. Bordiga, K. P. Lillerud, *J. Am. Chem. Soc.* **2008**, 130, 13850–13851.
- [21] K. S. Park, Z. Ni, A. P. Côté, J. Y. Choi, R. Huang, F. J. Uribe-Romo, H. K. Chae, M. O'Keeffe, O. M. Yaghi, *Proc. Natl. Acad. Sci. USA* **2006**, 103, 10186.
- [22] Z. Wei, Z.-Y. Gu, R. K. Arvapally, Y.-P. Chen, R. N. McDougald, J. F. Ivy, A. A. Yakovenko, D. Feng, M. A. Omary, H.-C. Zhou, *J. Am. Chem. Soc.* **2014**, 136, 8269–8276.
- [23] a) K. P. Carter, K. E. Thomas, S. J. A. Pope, R. J. Holmberg, R. J. Butcher, M. Murugesu, C. L. Cahill, *Inorg. Chem.* **2016**, 55, 6902–6915; b) K. P. Carter, S. J. A. Pope, M. Kalaj, R. J. Holmberg, M. Murugesu, C. L. Cahill, *Zeitschr. Anorg. Allg. Chemie* **2017**, 643, 1948–1955; c) K. P. Carter, R. G. Surbella III, M. Kalaj, C. L. Cahill, *Chem. Eur. J.* **2018**, 24, 12747–12756.
- [24] T. Tsuruoka, S. Furukawa, Y. Takashima, K. Yoshida, S. Isoda, S. Kitagawa, *Angew. Chem. Int. Ed.* **2009**, 48, 4739–4743; *Angew. Chem.* **2009**, 121, 4833–4837.
- [25] N. P. Martin, C. Volkringer, C. Falaise, N. Henry, T. Loiseau, *Cryst. Growth Des.* **2016**, 16, 1667–1678.

---

 Manuscript received: April 5, 2019

Accepted manuscript online: April 10, 2019

Version of record online: April 30, 2019